Supplementary Information

Hierarchical Nanoscale Multi-shell Au/CeO_2 Hollow Spheres

Pengfei, Xu, Ranbo Yu, Hao Ren, Lingbo Zong, Jun Chen, Xianran Xing*

Department of Physical Chemistry, School of Metallurgical and Ecological Engineering, University of Science and Technology Beijing, 100083, China
*Corresponding authors: ranboyu@ustb.edu.cn

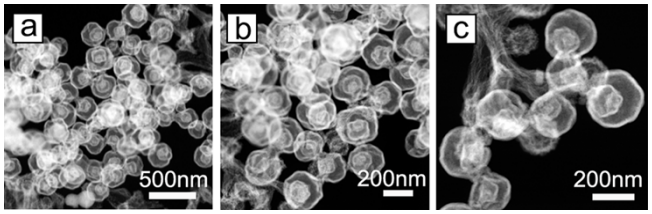

Fig. S1 HAADF STEM images of triple-shelled ceria hollow spheres. The calcination condition: at heat ramp rate of 10°C min^{-1} with 60 min holding 500°C.

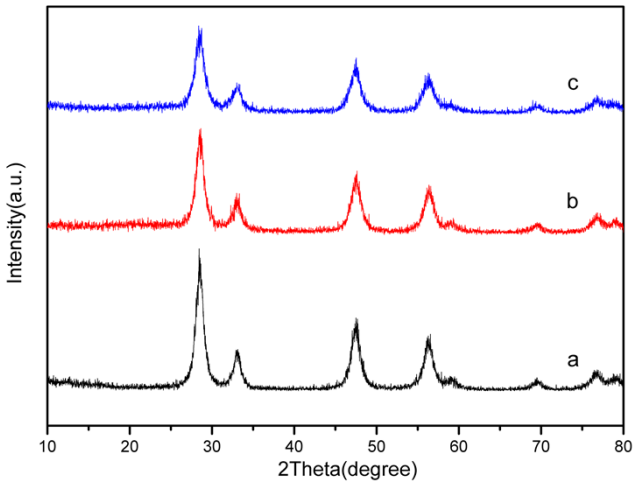

Fig. S2 XRD patterns of a) single-shell, b) double-shell and c) triple-shelled ceria hollow spheres.

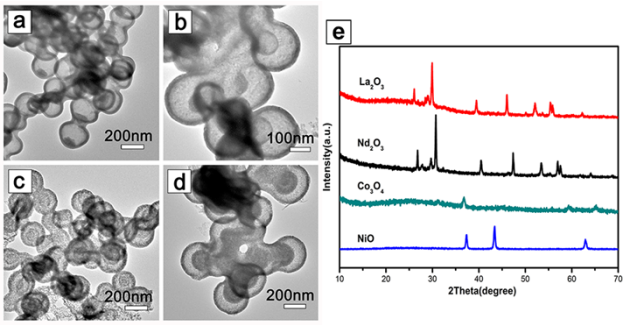

Fig. S3 a-d) Representative TEM images of various oxide multi-shelled hollow spheres: a) La_2O_3; b)Nd_2O_3; c) Co_3O_4; d) NiO. e) XRD patterns of the corresponding metal oxides.

When we substitute other metal ions (La^{3+}, Nd^{3+}, Co^{2+}, Ni^{2+}) for Ce^{3+} during hydrothermal process, corresponding multi-shelled metal oxides hollow spheres (La_2O_3, Nd_2O_3, Co_3O_4, NiO) were generated successfully as shown in Figure S3. These results confirmed the generality of our approach for hydrothermally enhanced synthesis of multi-shelled metal oxides hollow spheres.

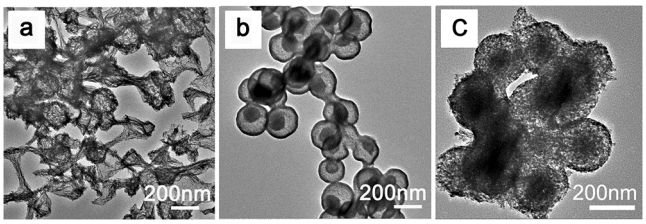

Fig. S4 TEM images of ceria obtained under different hydrothermal temperature when maintaining the same calcination condition. a) 120^{o}C, 6h; b) 160^{o}C, 6h; c) 180^{o}C, 6h. The calcination condition: at heat ramp rate of 2^{o}C min^{-1} with 60 min holding 500^{o}C.

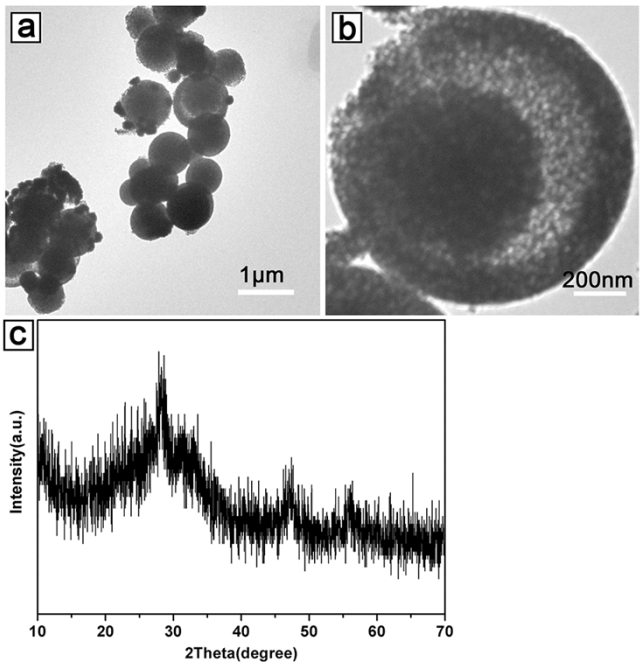

Fig. S5 a, b) TEM images and c) XRD patterns of ceria precursors obtained under the hydrothermal condition of 180^{o}C, 3h.

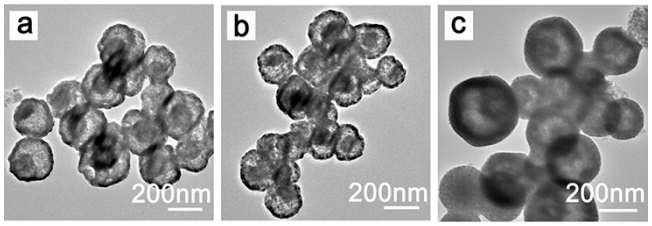

Fig. S6 TEM images of ceria obtained under the same calcination condition after the different hydrothermal time. a) 6h; b) 12h; c) 24h. The calcination condition: at heat ramp rate of 2^{o}C min^{-1} with 60 min holding 500^{o}C.

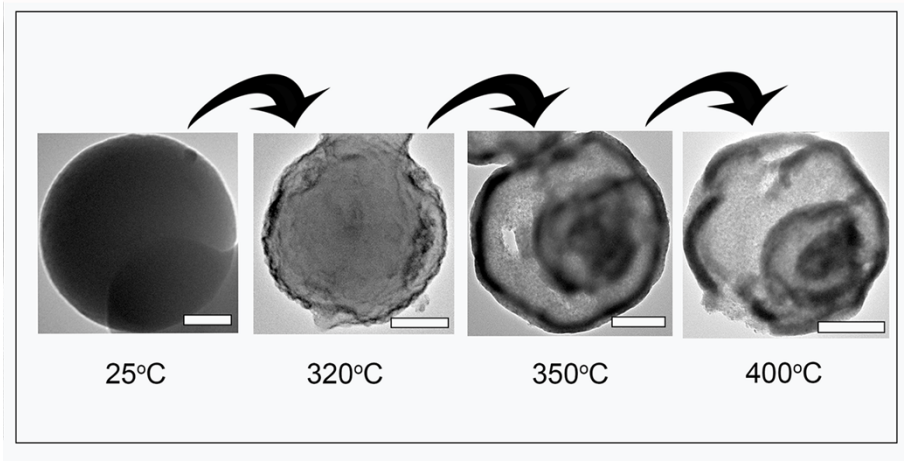

Fig. S7 The evolution of triple-shelled ceria by track of calcination process between 25°C and 400°C. The calcination condition: the heat ramp rate was set at 10°C min^{-1}. The scale bars: 50nm.

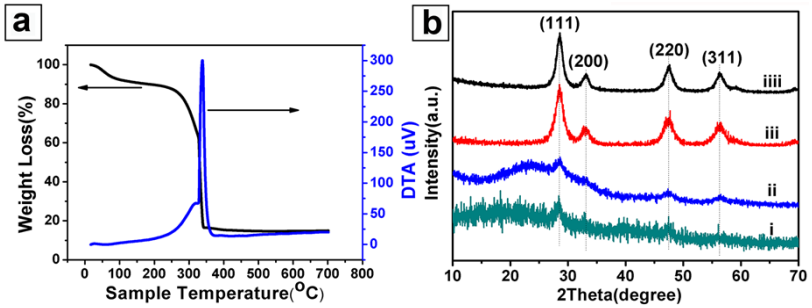

Fig. S8. a) TG-DTA curves of ACMSs; b) XRD patterns of immediate products obtained at different calcinations stage: i) before calcinations; ii) 320°C, 20min; iii) 350°C, 20min; iiii) 400°C, 20min.

Figure S8 gave the TG-DTA curves of ACMSs and XRD patterns of immediate products obtained at different calcinations stage. The two exothermal peaks centered at 320°C and 340°C appeared. And the XRD patterns showed the crystallization of cerium precursors distinctly happened in the range of 320°C~350°C. So it was inferred that the exothermal peak centered at 320°C originated from combustion heat of organic species while crystallization heat of ceria contributed to the exothermal peak centered at 340°C.

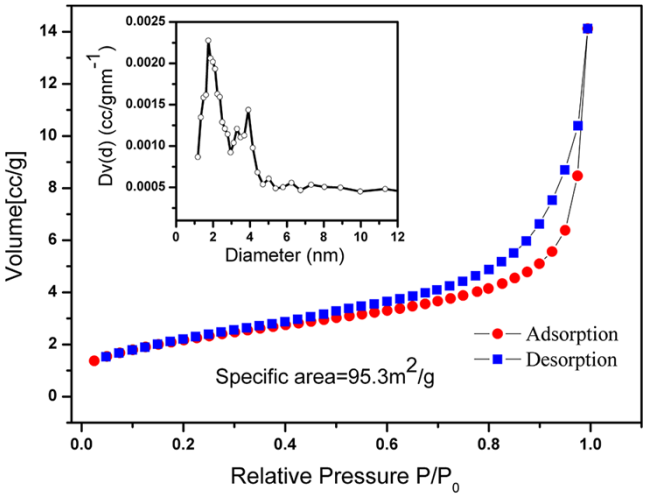

Fig. S9 The nitrogen adsorption-desorption isotherm curves of ceria hollow spheres with triple shell. Inset: the BJH pore size distribution of ceria hollow spheres with triple shell from the adsorption branch**.**

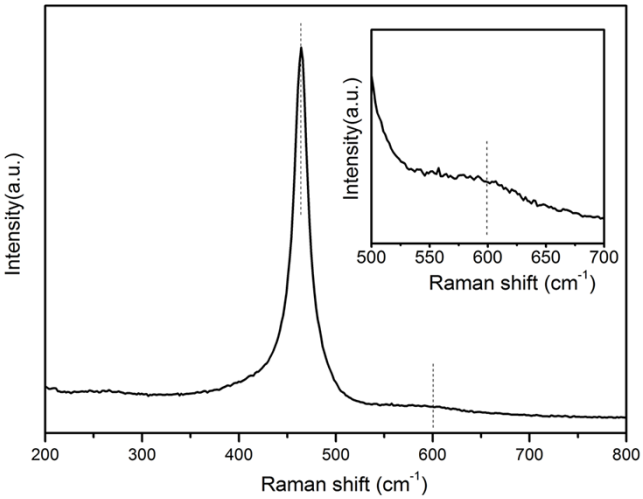

Fig. S10 Raman spectra of ceria hollow spheres with triple shell. Inset: the regional magnification.

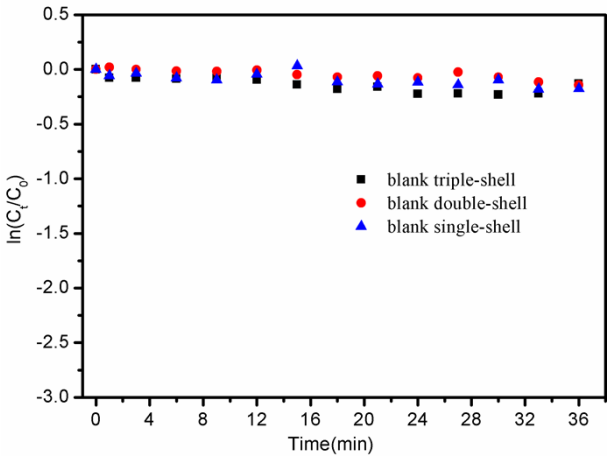

Fig. S11 Plots of $\ln(C_t/C_0)$ vs time by use of non-loaded MSCHSs (denoted as blank triple-shell, blank double-shell and blank single-shell).

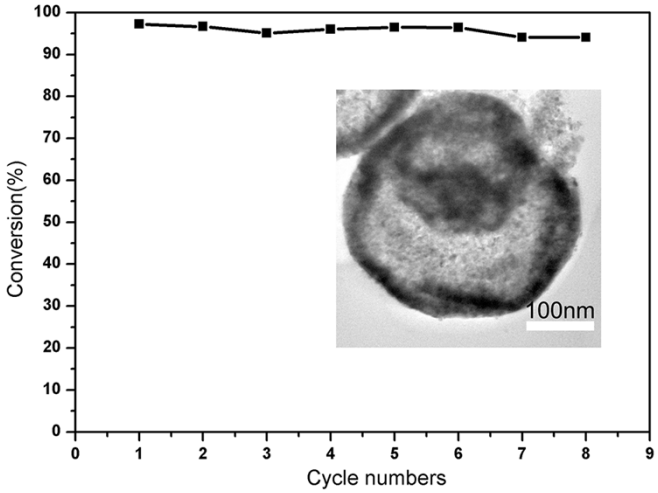

Fig. S12. Cycle stability of the triple-shell Au/CeO_2 hybrid catalyst. Inset: TEM image of the catalyst after 8 cycles.

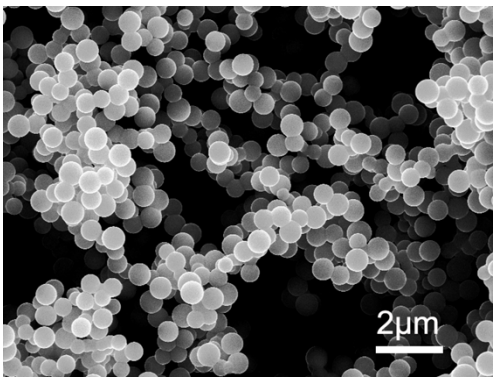

Fig. S13 Representative SEM images of as-synthesized carbonaceous spheres.